Table V. Selected Positional Parameters for the Cation in $[(TMT)Ru(H_2O)_3](OTf)_2$

	x/a	y/b	z/c
Ru	0.5623 (1)	-0.25	0.4577 (2)
O1A	0.7227 (7)	-0.25	0.421 (6)
O2A	0.597 (3)	-0.176 (1)	0.645 (3)
O1B	0.7195 (6)	-0.233 (1)	0.411 (3)
O2B	0.600 (2)	-0.210 (1)	0.692 (1)
O3B	0.593 (2)	-0.3437 (7)	0.589 (2)
S	0.3911 (4)	-0.25	0.4233 (8)
C1	0.466 (1)	-0.1863 (9)	0.331 (2)
C2	0.5361 (10)	-0.2140 (7)	0.221 (2)
C3	0.440 (2)	-0.1102 (9)	0.364 (3)
C4	0.602 (1)	-0.169 (1)	0.117 (2)

atoms and the CF_3 groups were refined with common isotropic thermal parameters and anisotropic thermal coefficients were refined for the remaining non-hydrogen atoms. Successful convergence was indicated by the maximum shift/error for the final cycle. The highest peaks in the final difference Fourier map were in the vicinity of the disordered fluorine atoms. A final analysis of variance between observed and calculated structure factors showed an inverse dependence on sin θ. Details of the crystallography are presented in Table IV. Selected atomic coordinates are given in Table V.

Acknowledgment. This research was supported by the National Science Foundation and in part the donors of the Petroleum Research Fund, administered by the American Chemical Society. Ruthenium trichloride was obtained from Johnson Matthey, Inc. Dr. John Lockemeyer is thanked for helpful discussions, and Dr. George Wagner is thanked for recording the CP-MAS NMR spectra. Dr. Bian Xiao Zhong gave us a generous sample of $[Ru(H_2O)_6][(OTs)_2$. Dr. P. Bernhard (Universität Bern) kindly provided us with his recently improved synthesis of this salt.

Supplementary Material Available: Tables of bond distances and angles, positional parameters, and thermal parameters (5 pages); a table of structure factors (6 pages). Ordering information is given on any current masthead page.

Mechanistic Studies of the Reductive Coupling of Carbon Monoxide in Seven-Coordinate Niobium(I) and Tantalum(I) Dicarbonyl Complexes

Raymond N. Vrtis, Shuncheng Liu, Ch. Pulla Rao, Simon G. Bott, and Stephen J. Lippard*

Department of Chemistry, Massachusetts Institute of Technology, Cambridge, Massachusetts 02139

Received March 12, 1990

The mechanism by which the two carbonyl ligands in the seven-coordinate complexes $[M(CO)_2(dmpe)_2Cl]$ [M = Ta, Nb; dmpe = 1,2-bis(dimethylphosphino)ethane] are reductively coupled has been elucidated. The first step involves two-electron reduction to afford the $[M(CO)_2(dmpe)_2]^-$ anion, the tantalum analogue of which was structurally characterized as the tetra-*n*-hexylammonium salt. The geometry of this anion is distorted octahedral with *cis*-carbonyl ligands. Reaction of the anion with 1 equiv of trialkylsilyl chloride yields the siloxycarbyne species $[M(\equiv COSiR_3)(CO)(dmpe)_2]$ (M = Ta or Nb), formed by electrophilic attack of the silyl halide on the carbonyl oxygen atom. The tantalum triisopropylsiloxycarbyne complex, the X-ray structural analysis of which is described, reacts with 1 equiv of trimethylsilyl chloride to afford the asymmetric acetylene complex, $[Ta\{Me_3SiOC\equiv COSi(i\text{-}Pr)_3\}(dmpe)_2Cl]$, which was also structurally characterized. The transition state between the carbyne and coupled products may be an η^2-ketenyl of the type $[Ta\{\eta^2\text{-}(O)\text{-}CCOSiR_3\}(dmpe)_2X]^-$ (X = halide). Such an assignment is supported by a series of experiments involving addition of different silyl halide reagents (Me_3SiX; X = Cl, I, OTf) to $(n\text{-}C_6H_{13})_4N[Ta(CO)_2(dmpe)_2]$. The generality of the reaction mechanism is discussed.

Introduction

Reaction chemistry that yields useful organic substrates starting from abundant C_1 precursors such as carbon monoxide has great potential value. Reduction of CO by alkali metals[1] or electrochemically[2] affords $M_2(C_2O_2)$ and higher oligomers from which a variety of organic products has been isolated.[1-3] The reductive coupling of CO has also been accomplished by using soluble transition, lanthanide, and actinide metal complexes.[4] As shown schematically in eqs 1 and 2, nearly all of these reactions are believed to proceed via the intra- or intermolecular coupling of oxocarbenes, with the carbonyl oxygen atoms ultimately bonded to the metal center(s).[5] Recently, however, theoretical calculations and experimental studies of the reaction of CO with $[Cp^*_2Hf(H)(CH_2CHMe_2)]$[6] have

(1) (a) Liebig, J. *Ann. Chem. Pharm.* **1834**, *11*, 182. (b) Joannis, A. *C. R. Hebd. Acad. Sci.* **1893**, *116*, 1518; **1914**, *158*, 874. (c) Pearson, T. G. *Nature* **1933**, *131*, 166. (d) Hackspill, L.; van Altane, L. A. *C. R. Hebd. Acad. Sci.* **1938**, *206*, 1818. (e) Scott, A. F. *Science* **1952**, *115*, 118. (f) Weiss, E.; Büchner, W. *Helv. Chim. Acta* **1963**, *46*, 2111; **1964**, *47*, 4157. (g) Weiss, E.; Büchner, W. Z. *Anorg. Allg. Chem.* **1964**, *330*, 251. (h) Weiss, E.; Büchner, W. *Chem. Ber.* **1965**, *98*, 126. (i) Ellis, J. E.; Fjare, K. L.; Hayes, T. G. *J. Am. Chem. Soc.* **1981**, *103*, 6100.

(2) (a) Silvestri, S.; Gambino, G.; Filardo, G.; Guainazzi, M.; Ercoli, R. *Gazz. Chim. It.* **1972**, *102*, 818. (b) Silvestri, S.; Gambino, G.; Filardo, G.; Spadaro, G.; Palmisano, L. *Electrochim. Acta* **1978**, *23*, 413. (c) Bockmair, G.; Fritz, H. P. *Z. Naturforsch. B.* **1975**, *30B*, 330. (d) Uribe, F. A.; Sharp, P. R.; Barb, A. J. *J. Electroanal. Chem.* **1983**, *152*, 173.

(3) (a) Büchner, W. *Helv. Chim. Acta* **1965**, *48*, 1229. (b) Barber, J. Ph.D. Thesis, Massachusetts Institute of Technology, Cambridge, 1981, Chapter III.

(4) For a review, see: Vrtis, R. N.; Lippard, S. J. *Israel J. Chem.*, in press.

(5) A notable exception is discussed in: Wayland, B. B.; Sherry, A. E.; Coffin, V. L. *J. Chem. Soc., Chem. Commun.* **1989**, 662.

0276-7333/91/2310-0275$02.50/0

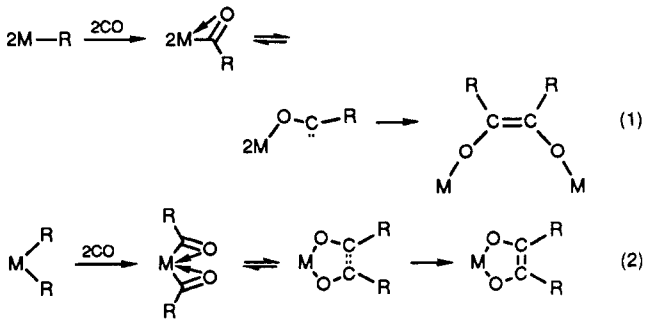

(1)

(2)

suggested that the reaction shown in eq 2 proceeds via initial reaction of CO with the MR_2 fragment, forming an η^2-ketone complex. This species then inserts a second CO into the ketone fragment followed by migration of an alkyl group to yield the observed product. Work by Rothwell et al.[7] has shown that the possibly related reductive coupling of isocyanides in early transition metal dialkyl aryl oxide complexes, $[(ArO)_nMR_2]$, proceeds via a bis(η^2-iminoacyl) complex.

Recently, we reported the reductive coupling of two CO ligands bound to tantalum or niobium in seven-coordinate complexes of the kind $[M(CO)_2(dmpe)_2Cl]$ [M = Ta (**1**) or Nb (**2**); dmpe = 1,2-bis(dimethylphosphino)ethane],[8] eq 3. The product of this reaction differs from those seen

$$[Ta(CO)_2(dmpe)_2Cl] \xrightarrow[(2)\ 2R_3SiX]{(1)\ 40\%\ Na/Hg} [Ta(R_3SiOCCOSiR_3)(dmpe)_2X] \quad (3)$$
$$\mathbf{1} \qquad\qquad X = Cl \text{ or } OTf$$

in almost all other examples of CO reductive coupling in that the oxygen atoms of the bis(trialkylsiloxy)acetylene ligand are not bound to an oxyphilic metal center; instead, they are bound to silyl groups. The difference in the bonding mode of the product in this reaction suggested a different reductive coupling reaction pathway in this system compared to those discussed above. Reported here are details of our mechanistic investigation of this chemistry, including crystal structure determinations of three compounds that lie along the pathway to reductive coupling. Preliminary aspects of this work have been communicated previously.[9]

Experimental Section

Materials. All reactions and manipulations were carried out either in a nitrogen-filled Vacuum Atmospheres drybox or under argon by using standard Schlenk techniques. All solvents were distilled under nitrogen from sodium benzophenone ketyl and stored over molecular sieves. Deuterated benzene was dried by passage through a column of alumina and stored over 3-Å molecular sieves. Deuterated tetrahydrofuran (THF-d_8) was dried by vacuum transfer from sodium benzophenone ketyl. Tetramethylsilane (Aldrich) was purified by vacuum transfer from calcium hydride. The starting materials $[Ta(CO)_2(dmpe)_2Cl]$ (**1**) and $[Nb(CO)_2(dmpe)_2Cl]$ (**2**) were synthesized by using modified literature procedures.[10] Forty percent sodium amalgam was prepared by a literature method.[11] Trimethylsilyl chloride (Me_3SiCl), trimethylsilyl iodide (Me_3SiI), trimethylsilyl trifluoromethanesulfonate (Me_3SiOTf), and triisopropylsilyl chloride (i-Pr_3SiCl) were obtained from Petrarch and used without further purification. Tetra-n-hexylammonium chloride $[(n\text{-}C_6H_{13})_4NCl]$ (Aldrich) was dried by heating the salt in an oil bath at 100 °C under vacuum for 12 h.

In Situ Preparation of $Na[Ta(CO)_2(dmpe)_2]$ (3a). A mixture of 0.1299 g (0.227 mmol) of $[Ta(CO)_2(dmpe)_2Cl]$ (**1**), excess 40% sodium amalgam, and 7 mL of THF was stirred under nitrogen for 5 h during which time the color changed from orange to red-brown. Filtration followed by removal of the THF in vacuo yielded 0.1175 g (92%) of $Na[Ta(CO)_2(dmpe)_2]$ (**3a**). The $^{31}P\{^1H\}$ NMR spectrum of an aliquot of the reaction mixture before the solvent was removed revealed no other phosphorus-containing species and no free dmpe. FTIR (KBr pellet) 2965 (m), 2922 (m), 2897 (s), 2800 (sh), 1663 (s), 1561 (s), 1415 (m), 1275 (m), 925 (s), 884 (sh), 696 (m), 627 (m), 579 (m) cm^{-1}; ^1H NMR (300 MHz, THF-d_8) δ 1.59 (d, 6 H, PCH_3, J_{P-H} = 2.1 Hz), 1.45 (d, 6 H, PCH_3, J_{P-H} = 2.1 Hz), 1.41 (d, PCH_3, 6 H, J_{P-H} = 3.3 Hz), 1.09 (d, 6 H, PCH_3, J_{P-H} = 1.8 Hz) ppm (resonances for the 8 methylene protons were too broad to observe); $^{31}P\{^1H\}$ NMR (121 MHz, THF, referenced to external 85% H_3PO_4) δ 22.6, 8.0 ppm; $^{13}C\{^1H\}$ NMR (75 MHz, THF-d_8) δ 253.5 (CO); 67.7 and 25.9 (dmpe) ppm.

Preparation of $(n\text{-}C_6H_{13})_4N[Ta(CO)_2(dmpe)_2]$ (3b). To a mixture of $[Ta(CO)_2(dmpe)_2Cl]$ (**1**), excess 40% sodium amalgam, and THF, prepared, stirred for 5 h, and filtered as described above, was added 0.3544 g (0.908 mmol) of $(n\text{-}C_6H_{13})_4NCl$. After 1 h of stirring, the color of the solution had changed from red-brown to deep red, at which time the THF was removed in vacuo. Extraction of the red product in 4 mL of Et_2O followed by cooling to −30 °F for 24 h yielded 0.0868 g (43%) of $(n\text{-}C_6H_{13})_4N[Ta(CO)_2(dmpe)_2]$ (**3b**). FTIR (KBr pellet) 2955 (m), 2924 (m), 2885 (m), 1705 (s), 1614 (s), 1487 (w), 1466 (w), 1415 (w), 1259 (w), 925 (m), 912 (sh), 894 (w), 875 (m), 696 (m), 619 (m) cm^{-1}; $^{31}P\{^1H\}$ NMR (121 MHz, THF, referenced to external 85% H_3PO_4) δ 23.3 (d, J_{PP} = 10 Hz), 9.7 (d, J_{PP} = 10 Hz) ppm. Anal. Calcd for $C_{38}H_{84}NO_2P_4Ta$: C, 51.17; H, 9.49; N, 1.57. Found: C, 50.81; H, 9.33; N, 1.50.

Reaction of $[Ta(CO)_2(dmpe)_2Cl]$ (1) with 1 Equiv of Sodium Naphthalenide. A solution of 0.151 mmol of sodium naphthalenide in 7 mL of THF was prepared by allowing 0.0193 g of naphthalene to react with an excess of sodium for a period of 12 h. The sodium naphthalenide was then added via pipet to a round-bottomed flask containing 0.0786 g (0.1372 mmol) of $[Ta(CO)_2(dmpe)_2Cl]$ (**1**) in 5 mL of THF. Upon addition of the sodium naphthalenide, there was an immediate color change from orange to red-brown. A ^{31}P NMR spectrum (121 MHz, THF, referenced to external 85% H_3PO_4) of this reaction solution revealed three resonances at 24.5, 22.5, and 8.0 ppm, arising from a mixture of **1** and **3a**.

Preparation of $[Ta\{\equiv COSi(i\text{-}Pr)_3\}(CO)(dmpe)_2]$ (4). A mixture of 0.1000 g (0.175 mmol) of $[Ta(CO)_2(dmpe)_2Cl]$ (**1**), 0.3291 g of 40% sodium amalgam, and 8 mL of THF was stirred under nitrogen in a flask for 4.5 h during which time the color changed from orange to red-brown. This mixture was then filtered, and 37 μL (0.173 mmol) of $(i\text{-}Pr)_3SiCl$ was added to the filtrate, causing a rapid color change from red-brown to plum-red. After $^1/_2$ h of continued stirring, the THF was removed in vacuo, leaving a viscous oil. The plum-red product was extracted into 5 mL of tetramethylsilane and the resulting solution filtered. Removal of the tetramethylsilane in vacuo yielded 0.1083 g (90.1%) of $[Ta\{\equiv COSi(i\text{-}Pr)_3\}(CO)(dmpe)_2]$ (**4**). FTIR (KBr pellet) 2960 (m), 2894 (m), 2865 (m), 1775 (s), 1736 (m), 1466 (w), 1416 (m), 1387 (w), 1306 (sh), 1269 (m), 1117 (w), 1074 (w), 1014 (w), 994 (w), 931 (s), 921 (s), 905 (sh), 883 (m), 829 (w), 780 (m), 713 (w), 690 (m), 628 (w) cm^{-1}; ^1H NMR (300 MHz, C_6D_6) δ 0.64

(6) (a) Hofmann, P.; Stauffert, P.; Frede, M.; Tatsumi, K. *Chem. Ber.* **1989**, *122*, 1559. (b) Roddick, D. N.; Bercaw, J. E. *Chem. Ber.* **1989**, *122*, 1579.

(7) (a) Chamberlain, L. R.; Durfee, L. D.; Fanwick, P. E.; Kobriger, L. M.; Latesky, S. L.; McMullen, A. K.; Steffy, B. D.; Rothwell, I. P.; Folting, K.; Huffman, J. C. *J. Am. Chem. Soc.* **1987**, *109*, 6068. (b) Durfee, L. D.; McMullen, A. K.; Rothwell, I. P. *J. Am. Chem. Soc.* **1988**, *110*, 1463. (c) Chamberlain, L. R.; Steffey, B. D.; Rothwell, I. P.; Huffman, J. C. *Polyhedron* **1989**, *8*, 341.

(8) (a) Bianconi, P. A.; Williams, I. D.; Engeler, M. P.; Lippard, S. J. *J. Am. Chem. Soc.* **1986**, *108*, 311. (b) Bianconi, P. A.; Vrtis, R. N.; Rao, Ch. P.; Williams, I. D.; Engeler, M. P.; Lippard, S. J. *Organometallics* **1987**, *6*, 1968.

(9) Vrtis, R. N.; Rao, Ch. P.; Warner, S.; Lippard, S. J. *J. Am. Chem. Soc.* **1988**, *110*, 2669.

(10) (a) Datta, S.; Wreford, S. S. *Inorg. Chem.* **1977**, *16*, 1134. (b) Burt, R. J.; Leigh, G. J.; Hughes, D. L. *J. Chem. Soc., Dalton Trans.* **1981**, 793. (c) Bianconi, P. A. Ph.D. Thesis, Massachusetts Institute of Technology, Cambridge, 1986, Chapter III.

(11) Fieser, L. F.; Fieser, M. In *Reagents for Organic Synthesis*; Wiley: New York, 1967; Vol. 1, p 1033.

(d, 3 H, PCH_3, J_{PH} = 3.2 Hz), 0.96 (d, 3 H, PCH_3, J_{PH} = 3.5 Hz), 1.50 (d, 3 H, PCH_3, J_{PH} = 4.3 Hz), 1.48 (d, 3 H, PCH_3, J_{PH} = 3.4 Hz), 1.4–1.20 (m, 35 H), 1.80 (d, 3 H, PCH_3, J_{PH} = 6.8 Hz), 1.84 (d, 3 H, PCH_3, J_{PH} = 6.9 Hz) ppm; ^{31}P NMR (161.9 MHz, C_6D_6, referenced to external 85% H_3PO_4) δ 25.4, 24.7, 11.7, −0.6 ppm; $^{13}C\{^1H\}$ NMR (100 MHz, C_6D_6) δ 253.15 (s, CO), 243.37 (s, ≡COSi) ppm. Anal. Calcd for $C_{23}H_{53}O_2P_4SiTa$: C, 39.77; H, 7.69; P, 17.84; Si, 4.04. Found: C, 38.92; H, 7.58; P, 17.60; Si, 4.26.

Preparation of [Nb{≡COSi(*i*-Pr)$_3$}(CO)(dmpe)$_2$] (5). The procedure used to prepare [Nb{≡COSi(*i*-Pr)$_3$}(CO)(dmpe)$_2$] (**5**) was the same as that described above for the tantalum analogue. A 0.101-g (0.208 mmol) portion of $[Nb(CO)_2(dmpe)_2Cl]$ (**2**), excess 40% sodium amalgam, and 8 mL of THF were used to form the anion $[Nb(CO)_2(dmpe)_2]^-$. Addition of 44 μL (0.206 mmol) of $(i\text{-Pr})_3SiCl$ yielded 0.1180 g (93.4%) of [Nb{≡COSi(*i*-Pr)$_3$}(CO)(dmpe)$_2$] (**5**). FTIR (KBr pellet) 2963 (s), 2894 (s), 2865 (s), 1781 (s), 1740 (s), 1466 (w), 1417 (m), 1388 (w), 1367 (w), 1294 (s), 1278 (s), 1119 (w), 1074 (w), 1014 (w), 995 (w), 932 (s), 883 (s), 749 (m), 713 (sh), 686 (m), 654 (w), 630 (m), 580 (w) cm^{-1}; ^1H NMR (400 MHz, C_6D_6) δ 0.62 (d, 3 H, PCH_3, J_{PH} = 2.5 Hz), 0.90 (d, 3 H, PCH_3, J_{PH} = 2.8 Hz), 1.41 (d, 3 H, PCH_3, J_{PH} = 4.3 Hz), 1.38 (d, 3 H, PCH_3, J_{PH} = 3.7 Hz), 1.31 (heptet, 3 H, CHMe, J_{HH} = 5.4 Hz), 1.27 (d, 18 H, CCH_3, J_{PH} = 5.4 Hz), 1.73 (d, 3 H, PCH_3, J_{PH} = 5.9 Hz), 1.68 (d, 3 H, PCH_3, J_{PH} = 5.8 Hz), 1.19 (d, 3 H, PCH_3, J_{PH} = 5.8 Hz), 1.15 (d, 3 H, PCH_3, J_{PH} = 5.8 Hz) ppm (resonances for the 8 methylene protons were too broad to observe). Anal. Calcd for $C_{23}H_{53}O_2P_4SiNb$: C, 45.54; H, 8.81. Found: C, 45.40; H, 8.23.

Reaction of (n-C_6H_{13})$_4$N[Ta(CO)$_2$(dmpe)$_2$] (3b) with 1 Equiv of Trimethylsilyl Chloride. A mixture of 0.1134 g (0.198 mmol) of $[Ta(CO)_2(dmpe)_2Cl]$ (**1**), excess 40% sodium amalgam, and 10 mL of THF was stirred in a pear-shaped flask for 6 h during which time the color of the solution gradually changed from orange to red–brown. The solution was filtered, and 0.3099 g (0.794 mmol) of $(n\text{-}C_6H_{13})_4NCl$ was added to the filtrate. The reaction mixture was allowed to stir for an additional 1 h after which time the THF was removed in vacuo. The red product was taken up in 15 mL of Et_2O and the solution filtered. The Et_2O was then removed in vacuo and $(n\text{-}C_6H_{13})_4N[Ta(CO)_2(dmpe)_2]$ (**3b**) was dissolved in 6 mL of THF containing 25 μL (0.197 mmol) of Me_3SiCl. The color of the solution changed from red to plum–red. A ^{31}P NMR spectrum of the reaction product revealed resonances at 24.7 (2 P), 12.2 (1 P), and −0.4 (1 P) ppm, consistent with the formulation [Ta(≡COSiMe$_3$)(CO)(dmpe)$_2$] in which two phosphorus atoms have identical chemical shifts.

Reaction of (n-C_6H_{13})$_4$N[Ta(CO)$_2$(dmpe)$_2$] (3b) with 1 Equiv of Trimethylsilyl Trifluoromethanesulfonate. A solution of 0.0707 g (0.123 mmol) of $[Ta(CO)_2(dmpe)_2Cl]$ (**1**), excess 40% sodium amalgam, and 7 mL of THF was stirred in a pear-shaped flask for 5 h during which time the color changed from orange to red–brown. This solution was filtered and 0.1931 g (0.495 mmol) of $(n\text{-}C_6H_{13})_4NCl$ was added to the filtrate. The resulting mixture was allowed to stir for an additional 1 h after which time the THF was removed in vacuo. The red product was extracted into 15 mL of Et_2O and the solution filtered. The Et_2O solution was then transferred into another pear-shaped flask, and the Et_2O was removed in vacuo. The product, $(n\text{-}C_6H_{13})_4N[Ta(CO)_2(dmpe)_2]$ (**3b**), was redissolved in 6 mL of dimethoxyethane, and 23 μL of Me_3SiOTf was added, causing an immediate color change from red to plum–red. A ^{31}P NMR spectrum of this reaction product revealed resonances at 24.7 (2 P), 12.2 (1 P), and −0.4 (1 P) ppm.

Reaction of (n-C_6H_{13})$_4$N[Ta(CO)$_2$(dmpe)$_2$] (3b) with 1 Equiv of Trimethylsilyl Iodide. A solution of 0.0779 g (0.136 mmol) of $[Ta(CO)_2(dmpe)_2Cl]$ (**1**), excess 40% sodium amalgam, and 6 mL of THF was stirred in a round-bottomed flask for 6 h during which time the color changed from orange to red–brown. This solution was then filtered and to the filtrate was added an excess of $(n\text{-}C_6H_{13})_4NCl$. The reaction was allowed to stir for an additional 2 h, after which time the red solution was again filtered and the THF removed in vacuo. The red product was extracted into 12 mL of Et_2O, the solution was filtered, and the Et_2O was removed in vacuo. $(n\text{-}C_6H_{13})_4N[Ta(CO)_2(dmpe)_2]$ (**3b**) was then dissolved in 5 mL of THF. To this solution was added 18.5 μL (0.136 mmol) of Me_3SiI, which resulted in a rapid color change from red to orange–green. The ^{31}P NMR spectrum of this mixture revealed three resonances at 23.3, 9.7 (**3b**), and 15.8 ([Ta(Me$_3$SiOCCOSiMe$_3$)(dmpe)$_2$I]) ppm.

Preparation of [Ta{Me$_3$SiOCCOSi(*i*-Pr)$_3$}(dmpe)$_2$Cl] (6). A mixture of 0.0938 g (0.164 mmol) of $[Ta(CO)_2(dmpe)_2Cl]$ (**1**), excess 40% sodium amalgam, and 6 mL of THF was stirred in a pear-shaped flask for 5 h, during which time the color changed from orange to red–brown. After filtration, 35 μL (0.164 mmol) of $(i\text{-Pr})_3SiCl$ was added to the filtrate. Over a period of 30 min, the color of the reaction mixture changed from red–brown to plum–red, after which time the THF was removed in vacuo. The plum–red product was then extracted into 5 mL of pentane and filtered. The pentane was removed in vacuo, and the plum–red product was redissolved in 8 mL of THF. To this solution, which contained [Ta{≡COSi(*i*-Pr)$_3$}(CO)(dmpe)$_2$] (**4**), was added 21 μL (0.165 mmol) of Me_3SiCl. The solution was stirred for 2 h, during which time the color changed from plum–red to green. The THF was removed in vacuo and the green product taken up in ~5 mL of pentane. After cooling to −30 °F for 24 h, 0.0619 g (47%) of [Ta{Me$_3$SiOCCOSi(*i*-Pr)$_3$}(dmpe)$_2$Cl (**6**) crystallized as a red solid. FTIR (KBr pellet) 2963 (s), 2944 (s), 2901 (s), 2864 (s), 1555 (m), 1464 (w), 1419 (m), 1291 (w), 1275 (w), 1251 (m), 1133 (s), 1058 (s), 941 (s), 925 (s), 990 (s), 843 (s), 730 (m), 696 (w), 678 (w) cm^{-1}; ^1H NMR (toluene-d_8, 300 MHz) δ 1.7–1.5 (br s, 2 H, PCH_2), 1.47 (br d, 24 H, PCH_3, $^2J_{PH}$ = 5.1 Hz), 1.25–1.4 (br s, 4 H, PCH_2), 1.21 (heptet, 3 H, CHMe, $^2J_{HH}$ = 7 Hz), 1.11 (d, 18 H, CCH_3, $^2J_{HH}$ = 7 Hz), 0.31 (s, 9 H, $SiCH_3$) ppm; ^{31}P NMR (toluene-d_8, 121 MHz, referenced to external 85% H_3PO_4) δ 25.6 ppm; $^{13}C\{^1H\}$ NMR (75 MHz, C_6D_6, 90% ^{13}C-enriched) δ 210.6 ($^2J_{PC}$ = 11, $^1J_{CC}$ = 6 Hz), 204.1 ($^2J_{PC}$ = 11, $^1J_{CC}$ = 6 Hz). Anal. Calcd for $C_{28}H_{62}ClO_2P_4Si_2Ta$: C, 38.88; H, 7.78; Cl, 4.41. Found: C, 39.37; H, 7.75; Cl, 4.70.

Spectral and Analytical Measurements. ^1H, ^{31}P, and ^{13}C NMR spectra were recorded on Varian XL-300 or XL-400 instruments. Infrared spectra were obtained on a Mattson Cygnus 100 FTIR spectrometer. Spin simulation was accomplished by using the iterative procedure in the FORTRAN program LAME, also known as LAOCOON, with magnetic equivalance added. This program is available on the Varian XL-300 instrument. Elemental analyses were performed by Analytical Laboratories, Engelskirchen, Germany, or Oneida Research Services, Whitesboro, NY.

Collection and Reduction of X-ray Data. (n-C_6H_{13})$_4$N[Ta(CO)$_2$(dmpe)$_2$] (3b). A red crystal of $(n\text{-}C_6H_{13})_4N[Ta(CO)_2(dmpe)_2]$ (**3b**) was obtained by cooling a concentrated solution of the compound in Et_2O to −20 °F. The crystal was mounted on a glass fiber under a stream of cold nitrogen with silicone grease. It was then transferred to the diffractometer and placed under a stream of nitrogen at −65 °C, at which temperature the crystal was maintained throughout the data collection. Examination on the diffractometer revealed $2/m$ Laue symmetry and systematic absences $h0l$, $h + l \neq 2n$, and $0k0$, $k \neq 2n$, consistent with the space group $P2_1/n$ (C_{2h}^5, No. 14, cell choice 4).[12a] Open counter ω scans of several strong, low-angle reflections showed no structure ($\Delta\bar{\omega}_{1/2}$ = 0.23°). Since there were no well-defined faces, an empirical absorption correction was applied based on ψ scans. Data collection proceeded via methods standard in our laboratory,[13] the details of which are given in Table I.

[Ta{≡COSi(*i*-Pr)$_3$}(CO)(dmpe)$_2$] (4). A deep red crystal of **4** was grown by slow evaporation of a tetramethylsilane solution at −30 °F and mounted under a nitrogen atmosphere in a Lindemann glass capillary with Apiezon grease. The crystal was judged acceptable on the basis of ω scans of several low-angle reflections which did not show any structure ($\Delta\bar{\omega}_{1/2}$ = 0.20°). Study on the diffractometer revealed $2/m$ Laue symmetry with systematic absences $0k0$, $k \neq 2n$, and $h0l$, $l \neq 2n$, consistent with the space group $P2_1/c$ (C_{2h}^5, No. 14, cell choice 1).[12a] Monitoring three intensity standards after every 60 min of exposure showed a linear decay of 20%, for which the data were corrected accordingly. An empirical absorption correction was applied based on azimuthal ψ scans. Data collection proceeded by methods standard in our laboratory,[13] the details of which are given in Table I.

(12) Hahn, T., Ed. *International Tables for Crystallography*; D. Reidel: Dordrecht, 1983; (a) pp 170–177, (b) pp 168–169, (c) pp 128–129.
(13) Silverman, L. D.; Dewan, J. C.; Giandomenico, C. M.; Lippard, S. J. *Inorg. Chem.* **1980**, *19*, 3379.

Table I. Experimental Details of the X-ray Diffraction Studies[a] of $(n\text{-}C_6H_{13})_4N[Ta(CO)_2(dmpe)_2]$ (3b), $[Ta(\equiv COSi(i\text{-}Pr)_3)(CO)(dmpe)_2]$ (4), $[Nb(\equiv COSi(i\text{-}Pr)_3)(CO)(dmpe)_2]$ (5), and $[Ta(Me_3SiOCCOSi(i\text{-}Pr)_3)(dmpe)_2Cl]$ (6)

	3b	4	5	6
	$C_{38}H_{84}NO_2P_4Ta$	$C_{23}H_{53}O_2P_4SiTa$	$C_{23}H_{53}O_2P_4SiNb$	$C_{26}H_{62}ClO_2P_4Si_2Ta$
a, Å	18.0779 (6)	9.836 (2)	9.821 (4)	15.566 (3)
b, Å	13.767 (1)	30.154 (4)	30.273 (7)	11.299 (2)
c, Å	19.127 (1)	12.248 (2)	12.236 (3)	21.490 (5)
β, deg	91.007 (4)	112.52 (2)	112.47 (2)	90.359 (8)
V, Å^3	4760 (1)	3356 (2)	3362 (3)	3780 (2)
temp, °C	−65	23	23	−70
fw	891.94	694.6	606.56	803.24
Z	4	4	4	4
ρ_{calcd}, g/cm^3	1.245	1.375	1.198	1.41
space group	$P2_1/n$	$P2_1/c$	$P2_1/c$	$P2/c$
data limits, deg	$2 < 2\theta \le 32$, $\pm h,\pm k,\pm l$ $32 < 2\theta < 50$, $+h,+k,\pm l$	$3 \le 2\theta \le 22$, $\pm h,\pm k,\pm l$ $22 < 2\theta < 49$, $+h,+k,\pm l$	$2 < 2\theta \le 20$, $+h,\pm k,\pm l$ $20 < 2\theta < 50$, $+h,+k,\pm l$	$1.5 < 2\theta < 55$, $\pm h,+k,+l$
transmission factors	0.72–1.00	0.69–1.00	0.93–1.00	0.90–1.00
crystal dimens, mm		0.15 × 0.32 × 0.48	0.18 × 0.35 × 0.40	0.40 × 0.32 × 0.30
linear abs coeff, cm^{-1}	24.4	34.8	5.9	31.9
no. of data collected	11294	7906	7608	9331
no. of unique data [$F > 6\sigma(F)$][b]	3962	3081	2028	6457
no. of params	355	279	280	325
R_1[c]	0.068	0.048	0.046	0.040
R_2[c]	0.090	0.060	0.056	0.058

[a] Data were collected by $2\theta/\omega$ scans on an Enraf-Nonius CAD-4F κ geometry diffractometer using Mo K$\bar{\alpha}$ radiation and a highly oriented graphite monochromator. [b] $\sigma(I) = (C + {}^1/_4(t_c/t_b)^2(b_1 + b_2) + (0.05I)^2)^{1/2}$ where C = total number of counts, t_c = time spent counting peak intensity, t_b = time spent counting one side of background, b_1 = high-angle background counts, b_2 = low-angle background counts, $I = C - {}^1/_2(t_c/t_b)(b_1 + b_2)$. [c] $R_1 = \sum||F_o| - |F_c||/\sum|F_o|$; $R_2 = [\sum w||F_o| - |F_c||^2/\sum w|F_o|^2]^{1/2}$, where $w = 1/\sigma^2(F_o)$.

$[Nb(\equiv COSi(i\text{-}Pr)_3)(CO)(dmpe)_2]$ (5). A deep red crystal of this compound was grown and mounted in a manner analogous that described above for 4. The crystal was judged acceptable on the basis of ω scans of several strong low-angle reflections, which did not show any structure ($\Delta\bar{\omega}_{1/2} = 0.23°$). Study on the diffractometer revealed the compound to be isomorphous with 4. The structure determination and refinement were carried out in space group $P2_1/c$ (C_{2h}^5, No. 14, cell choice 1).[12a] An empirical absorption correction was applied based on azimuthal ψ scans. Data collection proceeded by methods standard in our laboratory,[13] the details of which are given in Table I.

$[Ta(Me_3SiOCCOSi(i\text{-}Pr)_3)(dmpe)_2Cl]$ (6). A deep red crystal of 6 was grown from a concentrated pentane solution cooled to −30 °C. The crystal was mounted under a stream of cold nitrogen onto a glass fiber with silicone grease. It was then transferred to the diffractometer and cooled to −70 °C, at which temperature it was maintained throughout data collection. The crystal was judged acceptable on the basis of ω scans of several strong low-angle reflections, which did not show any structure ($\Delta\bar{\omega}_{1/2} = 0.31°$). Study on the diffractometer revealed $2/m$ Laue symmetry and systematic absences $h0l$, $l \neq 2n$, consistent with either the centrosymmetric space group $P2/c$ (C_{2h}^4, No. 13, cell choice 1)[12b] or the noncentrosymmetric space group Pc (C_s^2, No. 7, cell choice 1).[12c] A structure solution was attempted in both space groups. On the basis of lower R values and better refinement in the centrosymmetric space group, the former was taken as the correct choice. An empirical absorption correction was applied by using azimuthal ψ scans. Data collection proceeded by methods standard in our laboratory,[13] the details of which are given in Table I.

Structure Determination and Refinement. All calculations were carried out by using the TEXSAN program package.[14]

$(n\text{-}C_6H_{13})_4N[Ta(CO)_2(dmpe)_2]$ (3b). The position of the tantalum atom was determined from a Patterson synthesis, and all of the remaining non-hydrogen atoms were located from a series of difference Fourier maps. The large thermal parameters for the dmpe and some of the tetra-*n*-hexylammonium group carbon atoms may be due to unresolved disorder. All non-hydrogen atoms except the dmpe carbon atoms were assigned anisotropic thermal parameters. All hydrogen atoms were placed in calculated positions ($d_{C-H} = 0.95$ Å) and constrained to "ride" on the appropriate carbons with $B(H) = 1.2B_{eq}(C)$. The function minimized during refinement was $\sum w(|F_o| - |F_c|)^2$ where $w = 1/\sigma^2(F_o)$. Refinement in this manner yielded the residuals shown in Table I. The largest ratio of parameter shift to estimated standard deviation in the final cycle of refinement was 0.79. The largest peak in the difference Fourier map was 2.19 e$^-$/Å^3, located near P1 and C12. Final non-hydrogen atom positional and thermal parameters are given in Tables S1 and S2, respectively. Final hydrogen atom positional and thermal parameters along with a listing of observed and calculated structure factors are given in Tables S3 and S4, respectively.

$[Ta(\equiv COSi(i\text{-}Pr)_3)(CO)(dmpe)_2]$ (4). The position of the tantalum atom was determined from a Patterson synthesis, and all of the remaining non-hydrogen atoms were located from a series of difference Fourier maps. It became apparent that one of the isopropyl groups and the ethylene linkage on one dmpe were disordered. A suitable model was found in which two positions were refined at half occupancy for each of the disordered carbon atoms. All non-hydrogen atoms except the disordered carbon atoms were assigned anisotropic thermal parameters. All hydrogen atoms were placed in calculated positions ($d_{C-H} = 0.95$ Å) and constrained to "ride" on the appropriate carbons with $B(H) = 1.2B_{eq}(C)$. The function minimized during refinement was $\sum w(|F_o| - |F_c|)^2$ where $w = 1/\sigma^2(F_o)$. Refinement in this manner yielded the residuals shown in Table I. The largest ratio of parameter shift to estimated standard deviation in the final cycle of refinement was less than 0.002. The largest peak in the difference Fourier map was 0.86 e$^-$/Å^3, located 1.07 Å from the Ta atom. Final non-hydrogen atom positional and thermal parameters are given in Tables S5 and S6, respectively. Final hydrogen atom positional and thermal parameters along with a listing of observed and calculated structure factors are given in Tables S7 and S8, respectively.

$[Nb(\equiv COSi(i\text{-}Pr)_3)(CO)(dmpe)_2]$ (5). The position of the niobium atom was determined by a Patterson synthesis, and all of the remaining non-hydrogen atoms were located from a series of difference Fourier maps. Structure refinement proceeded smoothly, and all of the non-hydrogen atoms were assigned anisotropic thermal parameters. High-resolution Fourier maps, in which the grid spacing was 0.03 Å, in the vicinity of the methylene groups of the dmpe ligands did not show any resolved disorder despite the large thermal parameters. All hydrogen atoms were placed in calculated positions ($d_{C-H} = 0.95$ Å) and allowed to ride on the appropriate carbons with $B(H) = 1.2B_{eq}(C)$. The function minimized during refinement was $\sum w(|F_o| - |F_c|)^2$ where $w = 1/\sigma^2(F_o)$. Refinement in this manner yielded the R factors given in Table I. The largest ratio of parameter shift to estimated standard deviation in the final cycle of refinement was less than

(14) TEXSAN, a package of crystallographic programs supplied by the Molecular Structure Corporation. All computations were made on a DEC VAXstation II computer.

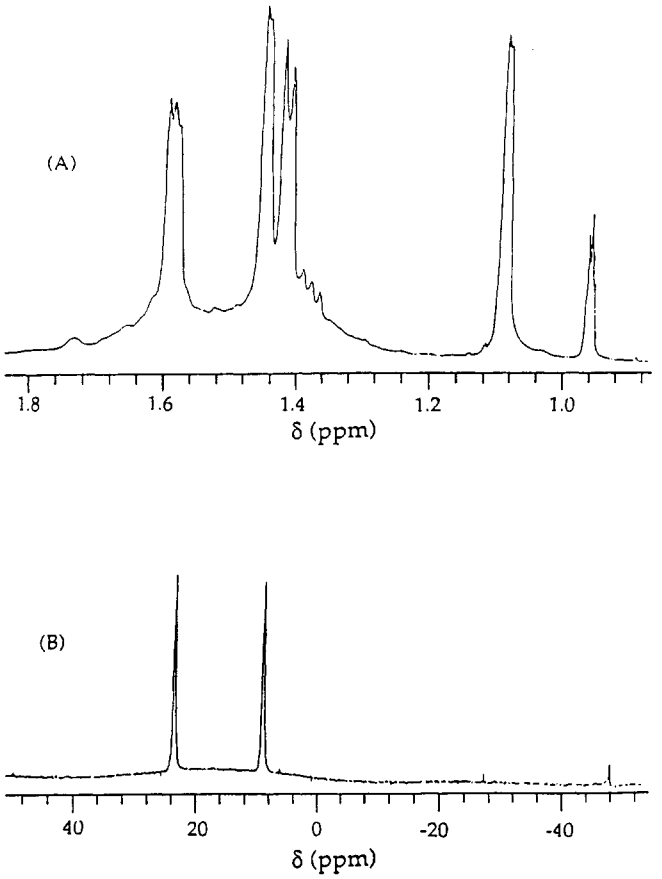

Figure 1. (A) ^1H and (B) ^{31}P NMR spectra of $Na[Ta(CO)_2(dmpe)_2]$ (**3a**).

0.009. The largest peak in the difference Fourier map was 0.43 $e^-/Å^3$, located 1.18 Å from the niobium atom. Final non-hydrogen atom positional and thermal parameters are given in Tables S9 and S10, respectively. Final hydrogen atom positional and thermal parameters along with a listing of observed and calculated structure factors are given in Tables S11 and S12, respectively.

$[Ta\{Me_3SiOCCOSi(i\text{-}Pr)_3\}(dmpe)_2Cl]$ (6). The position of the tantalum atom was determined from a Patterson synthesis, and all of the remaining non-hydrogen atoms were located from a series of difference Fourier maps. All of the non-hydrogen atoms were assigned anisotropic thermal parameters. All the hydrogen atoms were placed in calculated positions (d_{C-H} = 0.95 Å) and constrained to ride on the appropriate carbons with $B(H) = 1.2B_{eq}(C)$. The function minimized during refinement was $\sum w(|F_o| - |F_c|)^2$ where $w = 1/\sigma^2(F_o)$. Refinement in this manner yielded the residuals given in Table I. The largest ratio of parameter shift to estimated standard deviation in the final cycle of refinement was 0.02, and the largest peak in the difference Fourier map was 1.60 $e^-/Å^3$, located near the tantalum center. Final non-hydrogen atom positional and thermal parameters are given in Tables S13 and S14, respectively. Final hydrogen atom positional and thermal parameters along with a listing of observed and calculated structure factors are given in Tables S15 and S16, respectively.

Results

Two-Electron Reduction of $[Ta(CO)_2(dmpe)_2Cl]$ (1) To Form $[Ta(CO)_2(dmpe)_2]^-$ (3a or 3b). When the compound $[Ta(CO)_2(dmpe)_2Cl]$ (1) was allowed to react with a strong reducing agent such as 40% sodium amalgam, two-electron reduction occurred with loss of chloride to yield the anion $[Ta(CO)_2(dmpe)_2]^-$. The proton and phosphorus NMR spectra of $Na[Ta(CO)_2(dmpe)_2]$ (**3a**) are shown in Figure 1. This anion is very air- and water-sensitive and if the solvent is not rigorously dried will react with traces of water to form the known complex $[TaH(CO)_2(dmpe)_2]$.[15] This reaction does not pose a problem in the preparation of the anion, however, since prolonged reaction times and excess reducing agent eventually convert the hydride into the desired product.

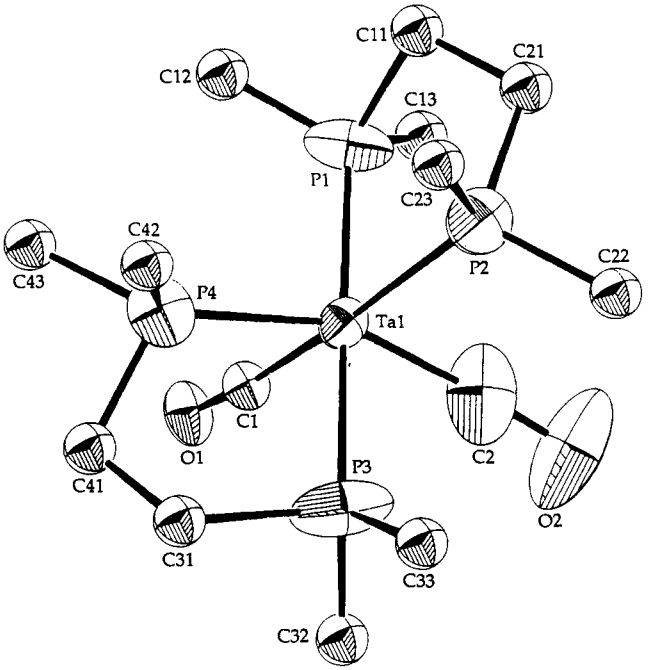

Figure 2. Structure of $[Ta(CO)_2(dmpe)_2]^-$ anion in **3b**. For clarity, methyl and methylene carbon atoms are depicted as spheres with B = 5.0 Å^2, while all other atoms are shown with 30% probability anisotropic thermal ellipsoids.

X-ray diffraction studies were performed on a suitable crystal of the anion isolated as the tetra-*n*-hexylammonium salt (**3b**). The structure is illustrated in Figure 2. The tantalum atom is in a distorted octahedral environment with the two carbonyl groups cis to one another. Distortions from an idealized octahedral geometry[16] arise mainly from the small bite angles (~78°) of the two chelating dmpe ligands. The cis arrangement of CO ligands is in accord with extended Hückel molecular orbital calculations, indicating the preferred geometry of 18-electron octahedral complexes containing strong π-acid and π-donor ligands.[17a]

Selected bond lengths and angles for **3b** are summarized in Table II. The Ta1–P1 bond is unexpectedly, but significantly, shorter than the other three Ta–P distances. This shortening may be the result of unresolved disorder or internal ligand packing interactions, which open the angles involving the Ta and P1 bond, as can be seen by examination of Figure 2 and Table II. The values of 1.99 (1) and 1.92 (3) Å for the Ta1–C1 and Ta1–C2 bond lengths, respectively, are reasonable for terminal carbonyl groups.[17b,c] Other features of the geometry are reasonable, given the low precision of the structure determination. A striking property of the anion is the abnormally low ν_{CO} stretching frequencies of 1663 and 1561 cm^{-1} for **3a** and 1705 and 1614 cm^{-1} for **3b** (Figure 3A). The difference in ν_{CO} between **3a** and **3b** can be attributed to the increased interaction of the stronger Lewis acid, sodium, with the carbonyl oxygen atoms in **3a**. The low CO stretching

(15) (a) Meakin, P.; Guggenberger, L. J.; Tebbe, F. N.; Jesson, J. P. *Inorg. Chem.* **1974**, *13*, 1025. (b) Tebbe, F. N. *J. Am. Chem. Soc.* **1973**, *95*, 5823.

(16) Kepert, D. L. *Inorganic Stereochemistry*; Springer-Verlag: Berlin, 1982.

(17) (a) Mingos, D. M. P. *J. Organomet. Chem.* **1979**, *179*, C29. (b) Bellard, S.; Rubison, K. A.; Sheldrick, G. M. *Acta Crystallogr.* **1979**, *B35*, 271. (c) Wilson, R. D.; Bau, R. *J. Am. Chem. Soc.* **1974**, *96*, 7601.

Table II. Interatomic Distances (Å) and Angles (deg) for $(n\text{-}C_6H_{13})_4N[Ta(CO)_2(dmpe)_2]$ (3b)[a]

Bond Lengths					
Ta1-C1	1.99 (1)	C2-O2	1.27 (3)	Ta1-P2	2.522 (5)
Ta1-C2	1.92 (3)	Ta1-P4	2.482 (6)	Ta1-P3	2.493 (8)
C1-O1	1.19 (2)	Ta1-P1	2.361 (6)		

Bond Angles			
C1-Ta1-C2	92.5 (8)	C2-Ta1-P3	79 (1)
O1-C1-Ta1	174 (1)	C2-Ta1-P4	156 (1)
O2-C2-Ta1	174 (3)	P4-Ta1-P1	86.3 (4)
C1-Ta1-P1	91.0 (5)	P4-Ta1-P2	100.1 (2)
C1-Ta1-P2	169.8 (4)	P4-Ta1-P3	77.4 (3)
C1-Ta1-P3	91.7 (5)	P1-Ta1-P2	80.0 (2)
C1-Ta1-P4	86.3 (4)	P1-Ta1-P3	177.2 (2)
C2-Ta1-P1	102 (1)	P2-Ta1-P3	97.4 (2)
C2-Ta1-P2	84.8 (7)		

	intraligand geometry		
bond or angle	min	max	mean
P-C	1.66 (5)	2.11 (4)	1.84 (4)
(P)C-C(P)			1.55 (5)
C-N	1.51 (2)	1.53 (2)	1.52 (2)
C-C	1.19 (4)	1.63 (4)	1.47 (3)
Ta-P-C	104 (1)	127 (1)	119 (1)
C-P-C	93 (2)	105 (2)	99 (2)
P-C-C	103 (3)	111 (3)	107 (3)
N-C-C	112 (1)	117 (1)	115 (1)
C-N-C	106 (1)	113 (1)	110 (1)
C-C-C	110 (1)	118 (5)	114 (2)

[a] Numbers in parentheses are estimated standard deviations in the last digit(s) given. Standard deviations quoted for the mean values are the average deviations for the individual values. See Figure 2 for atom-labeling scheme.

frequencies in both anions indicate significant M → CO π-backbonding, which is also reflected in the ^{13}C NMR chemical shift of 253.5 ppm observed for **3a**. The ^{31}P NMR spectra in THF exhibit two resonances at 22.6 and 8.0 ppm for **3a** and at 23.3 and 9.7 ppm for **3b**, with small cis coupling constants.

Reaction of $Na[M(CO)_2(dmpe)_2]$ (M = Ta or Nb) with 1 Equiv of Triisopropylsilyl Chloride. One equivalent of $(i\text{-}Pr)_3SiCl$ reacts with $Na[M(CO)_2(dmpe)_2]$ (M = Ta or Nb), generated in situ in THF, to yield the carbyne complex $[M\{\equiv COSi(i\text{-}Pr)_3\}(CO)(dmpe)_2]$ (M = Ta (**4**) or Nb (**5**)). The structure of **4** is shown in Figure 4. In this molecule, one of the isopropyl groups and one of the ethylene linkages on the dmpe are disordered. The nature of the disorder in the ethylene linkage is illustrated in the diagram

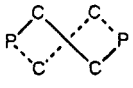

Selected bond lengths and angles for **4** [and the niobium analogue **5**, in square brackets] are given in Table III. As in **3b**, the environment about the tantalum atom in **4** (and the niobium atom in **5**) can be described as distorted octahedral.[16] The 1.85-Å Ta–C2 bond length in **4** is identical with the value reported for the alkylidyne complex $[Ta(\equiv CPh)(\eta^5\text{-}C_5H_5)(PMe_3)Cl]$[18] and appreciably shorter than the values of 2.01–2.03 or 2.25–2.32 Å found in tantalum alkylidene and alkyl complexes, respectively.[19] The C–$OSiR_3$ bond distance of 1.34 (2) Å is significantly longer than the values of 1.17 (1) and 1.20 (2) Å for the terminal carbonyl ligands in **4** and **5**, respectively. In addition, the Ta–P bond trans to the $Ta\equiv COSi(i\text{-}Pr)_3$ moiety is 0.13 Å longer than the average cis Ta–P bond distance. These

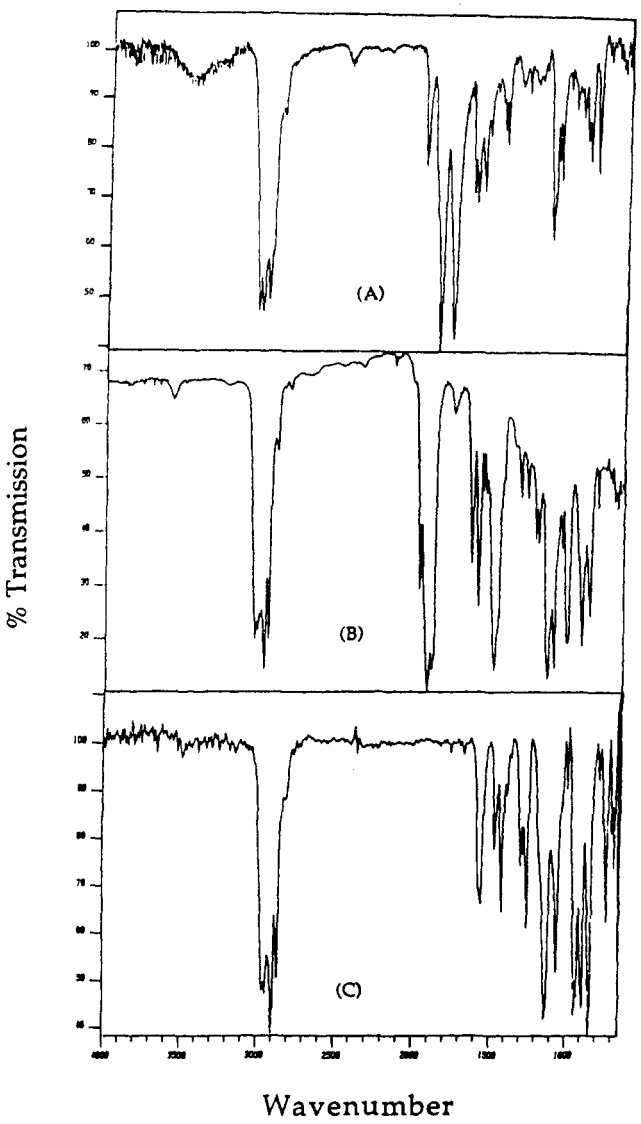

Figure 3. FTIR spectra of (A) $(n\text{-}C_6H_{13})_4N[Ta(CO)_2(dmpe)_2]$ (**3b**), (B) $[Ta\{\equiv COSi(i\text{-}Pr)_3\}(CO)(dmpe)_2]$ (**4**), and (C) $[Ta\{Me_3SiOCCOSi(i\text{-}Pr)_3\}(dmpe)_2Cl]$ (**6**) in KBr pellets.

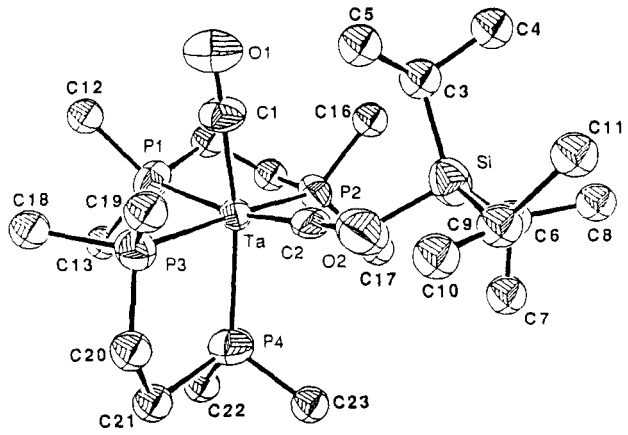

Figure 4. Structure of $[Ta\{\equiv COSi(i\text{-}Pr)_3\}(CO)(dmpe)_2]$ (**4**). For clarity, methyl and methylene carbon atoms are depicted as spheres with B = 5.0 Å^2, and only one orientation of a disordered isopropyl fragment and ethylene linker chain is drawn. All other atoms show anisotropic thermal ellipsoids at 40% probability.

(18) McLain, S. J.; Wood, C. D.; Messerle, L. W.; Schrock, R. R.; Hollander, F. J.; Youngs, W. J.; Churchill, M. R. *J. Am. Chem. Soc.* **1978**, *100*, 5962.

(19) (a) Gibson, V. C.; Grebenik, P. D.; Green, M. L. H. *J. Chem. Soc., Chem. Commun.* **1983**, 1101. (b) Guggenberger, L. J.; Schrock, R. R. *J. Am. Chem. Soc.* **1975**, *97*, 6578. (c) Schrock, R. R.; Messerle, L. W.; Wood, C. D.; Guggenberger, L. J. *J. Am. Chem. Soc.* **1978**, *100*, 3793. (d) Green, M. L. H.; Hare, P. M.; Bandy, J. A. *J. Organomet. Chem.* **1987**, *330*, 61.

Table III. Interatomic Distances (Å) and Angles (deg) for [Ta{≡COSi(*i*-Pr)$_3$}(CO)(dmpe)$_2$] (4) [and the Niobium Analogue 5 in Square Brackets][a]

Bond Lengths

Ta1-C2	1.85 (1) [1.88 (1)]	O2-C2	1.34 (2) [1.34 (1)]	Ta1-P3	2.490 (4) [2.505 (3)]
Ta1-C1	2.00 (2) [2.01 (1)]	Ta1-P1	2.636 (4) [2.668 (3)]	Ta1-P4	2.538 (4) [2.574 (3)]
O1-C1	1.20 (2) [1.17 (1)]	Ta1-P2	2.505 (4) [2.531 (3)]		
		Si1-O2	1.69 (1) [1.680 (8)]		

Bond Angles

C2-O2-Si1	128 (1) [126.9 (7)]	C1-Ta1-P2	94.9 (4) [94.5 (3)]
O1-C1-Ta1	176 (1) [178 (1)]	C1-Ta1-P3	89.5 (4) [89.1 (3)]
O2-C2-Ta1	172 (1) [172.7 (8)]	C1-Ta1-P4	167.5 (4) [166.8 (3)]
C2-Ta-C1	88.5 (6) [87.9 (5)]	P2-Ta1-P1	77.2 (1) [76.8 (1)]
C2-Ta1-P1	168.3 (5) [168.5 (3)]	P2-Ta1-P4	97.6 (1) [98.7 (1)]
C2-Ta1-P2	96.1 (5) [94.5 (3)]	P3-Ta1-P1	98.5 (1) [99.0 (1)]
C2-Ta1-P3	88.9 (5) [89.1 (3)]	P3-Ta1-P2	173.4 (1) [174.0 (1)]
C2-Ta1-P4	90.6 (4) [90.8 (3)]	P3-Ta1-P4	78.0 (2) [77.7 (1)]
C1-Ta1-P1	82.6 (5) [82.9 (3)]	P4-Ta1-P1	99.7 (2) [99.7 (1)]

	intraligand geometry		
bond or angle	min	max	mean
P-C	1.78 (2) [1.77 (1)]	1.99 (5) [1.87 (1)]	1.86 (2) [1.82 (1)]
Si-C	1.87 (2) [1.85 (2)]	1.93 (2) [1.87 (1)]	1.89 (2) [1.86 (2)]
(Si)C-C	1.38 (4) [1.32 (2)]	1.61 (3) [1.50 (2)]	1.50 (4) [1.45 (2)]
(P)C-C(P)			1.50 (4) [1.41 (2)]
M-P-C	104 (2) [105.7 (4)]	127.0 (8) [127.5 (6)]	116.8 (8) [117.2 (5)]
C-P-C	82 (2) [98.5 (6)]	117 (2) [102.6 (8)]	100 (1) [100.6 (7)]
P-C-C	106 (3) [111.9 (8)]	115 (3) [125 (1)]	112 (2) [116.4 (9)]
O-Si-C	100.3 (8) [100.8 (6)]	106.8 (7) [107.7 (8)]	104.0 (8) [105.1 (6)]
C-Si-C	110 (1) [112.7 (7)]	119 (1) [114 (1)]	114 (1) [113.4 (8)]
Si-C-C	107 (3) [111 (1)]	120 (2) [124 (1)]	114 (2) [117 (1)]
C-C-C	95 (3) [109 (2)]	139 (3) [119 (2)]	115 (3) [114 (2)]

[a] Numbers in parentheses are estimated standard deviations in the last digit(s) given. Standard deviations quoted for the mean values are the average deviations for the individual values. Atom labels are given in Figure 4.

structural features support the assignment of **4** and **5** as siloxycarbynes.

The $^{31}P\{^1H\}$ NMR spectrum of **4** dissolved in benzene-d_6 is displayed in Figure 5A. Four different phosphine chemical environments are revealed, in agreement with the solid-state geometry observed in the crystal structure. The ^{31}P splitting pattern observed can be fit as an ABMX pattern, as shown in Figure 5B. The coupling constants used for the simulation are J_{AB} = 32, J_{AM} = 12, J_{AX} = 13, J_{BM} = 19, J_{BX} = 16, and J_{MX} = 23 Hz. The $^{13}C\{^1H\}$ NMR spectrum of **4** consists of two resonances at 253 and 243 ppm, both of which fall within the range normally observed for terminal carbonyl ligands.[20] Because the chemical shift of the downfield resonance is coincident with that observed for the CO ligands in Na[Ta(CO)$_2$(dmpe)$_2$] (**3a**), however, it is tentatively assigned to the terminal carbonyl.

The M≡C stretching frequency of 1466 cm^{-1} observed in the FTIR spectra of both **4** (Figure 3B) and **5** is within the range usually reported for terminal carbynes.[21] The appearance of two stretching frequencies for the terminal carbonyl is unexpected; however, the bands at 1736 and 1740 cm^{-1} seen for **4** and **5**, respectively, may be due to an impurity such as the hydride complex [TaH(CO)$_2$(dmpe)$_2$], which exhibits a ν_{CO} band at 1740 cm^{-1}.[15] The formation of this compound is observed during the synthesis of **3a** owing to reaction with trace amounts of water.

Reaction of [Ta{≡COSi(*i*-Pr)$_3$}(CO)(dmpe)$_2$] (4) with 1 Equiv of Trimethylsilyl Chloride. This reaction yields the asymmetric disiloxyacetylene complex [Ta{Me$_3$SiOCCOSi(*i*-Pr)$_3$}(dmpe)$_2$Cl] (**6**), an ORTEP diagram of which is shown in Figure 6. Selected bond lengths and angles are summarized in Table IV. The geometry about the tantalum center in **6** is distorted octahedral[16] with the chloride atom and the midpoint of the acetylene ligand occupying the axial positions. Distortion from octahedral angles is again a consequence of the small bite angle of the dmpe ligands. The geometry of the coordinated acetylene is similar to that of other structurally characterized, four-electron-donating alkyne complexes, a point discussed

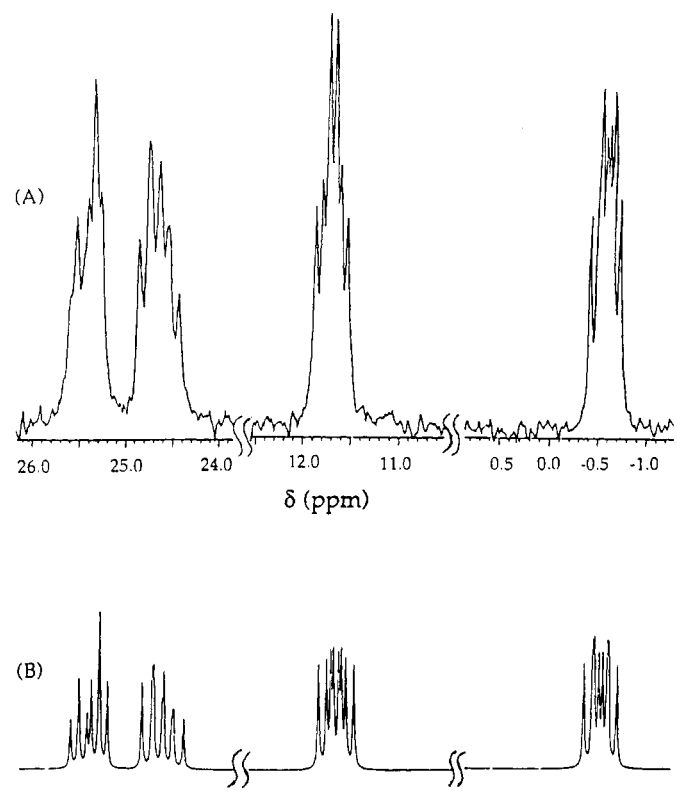

Figure 5. ^{31}P NMR spectrum in benzene-d_6 (A) and simulated spectrum (B) of [Ta{≡COSi(*i*-Pr)$_3$}(CO)(dmpe)$_2$] (**4**).

(20) Mann, B. E.; Taylor, B. F. In *^{13}C NMR Data for Organometallic Compounds*; Academic Press: New York, 1981.
(21) Kim, H. P.; Angelici, R. J. In *Advances in Inorganic Chemistry*; Academic Press: New York, 1987; Vol. 27.

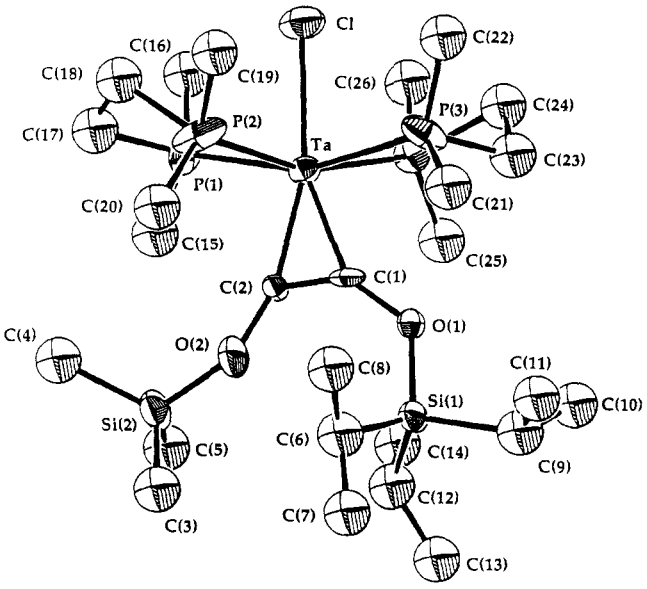

Figure 6. Structure of [Ta{$Me_3SiOCCOSi(i\text{-}Pr)_3$}$(dmpe)_2Cl$] (**6**). For clarity, methyl, methylene, and the carbon atoms on the silyl groups are depicted as spheres with $B = 5.0$ Å^2, whereas all other atoms show anisotropic thermal ellipsoids at 40% probability.

Table IV. Interatomic Distances (Å) and Angles (deg) for [Ta{$Me_3SiOCCOSi(i\text{-}Pr)_3$}$(dmpe)_2Cl$] (6)[a]

Bond Distances					
Ta-C2	2.086 (5)	Ta-P3	2.542 (2)	O1-C1	1.379 (7)
Ta-C1	2.134 (5)	Si1-O1	1.627 (4)	O2-C2	1.371 (6)
Ta-P1	2.532 (2)	Ta-P4	2.521 (2)	C1-C2	1.322 (7)
Ta-P2	2.509 (2)	Ta-C1	2.558 (2)	Si2-O2	1.666 (4)

Bond Angles			
C2-Ta-C1	36.5 (2)	O2-C2-Ta	150.9 (4)
C2-Ta-P2	109.1 (2)	C1-C2-Ta	73.7 (3)
C2-Ta-P4	88.5 (2)	C1-C2-O2	135.3 (5)
C2-Ta-P1	122.1 (1)	O1-C1-Ta	162.2 (4)
C2-Ta-P3	78.9 (1)	C2-C1-Ta	69.8 (3)
C2-Ta-C1	158.5 (2)	C2-C1-O1	127.2 (5)
C1-Ta-P2	91.8 (1)	C2-O2-Si2	131.0 (3)
C1-Ta-P4	107.2 (1)	C1-O1-Si1	151.7 (4)
C1-Ta-P1	87.9 (1)	P2-Ta-P4	160.80 (6)
C1-Ta-P3	113.3 (1)	P2-Ta-C1	79.48 (6)
C1-Ta-C1	164.9 (2)	P3-Ta-C1	80.42 (6)
P1-Ta-C1	78.38 (7)	P4-Ta-Cl	81.37 (6)
P1-Ta-P3	158.77 (6)	P4-Ta-P3	77.08 (7)
P2-Ta-P1	78.88 (8)	P4-Ta-P1	98.69 (6)
		P2-Ta-P3	98.21 (8)

	intraligand geometry		
bond or angle	min	max	mean
P-C	1.78 (1)	1.95 (1)	1.838 (9)
(P)C-C(P)			1.47 (2)
Ta-P-C	107.2 (3)	121.8 (3)	116.6 (3)
C-P-C	97.8 (7)	105.8 (5)	101.5 (5)
P-C-C	111.0 (8)	114.3 (8)	112.4 (8)
Si-C	1.846 (8)	1.900 (6)	1.867 (7)
(Si)C-C	1.50 (1)	1.534 (9)	1.516 (9)
O-Si-C	103.8 (2)	114.0 (3)	109.0 (3)
C-Si-C	106.7 (4)	114.2 (3)	109.9 (4)
Si-C-C	112.1 (4)	115.9 (4)	113.9 (4)
C-C-C	110.2 (5)	111.3 (6)	110.8 (6)

[a] Numbers in parentheses are estimated standard deviations in the last digit(s) given. Standard deviations quoted for the mean values are the average deviations for the individual values. Atom labels are defined in Figure 6.

in detail elsewhere.[8] The C-C distance of 1.322 (7) Å is similar to those in related bis(trimethylsiloxy)acetylene complexes [M($Me_3SiOCCOSiMe_3$)$(dmpe)_2X$] (M = Ta, X = Cl, OTf; M = Nb, X = Cl).[8] Unlike the latter molecules,

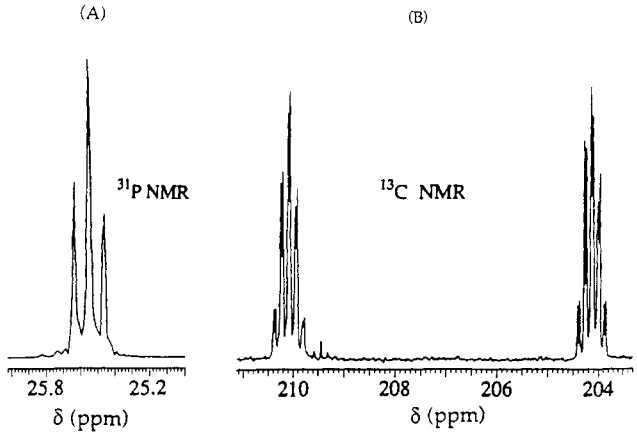

Figure 7. (A) ^{31}P and (B) ^{13}C NMR spectra of ^{13}C-enriched [Ta{$Me_3SiOCCOSi(i\text{-}Pr)_3$}$(dmpe)_2Cl$] (**6**).

however, the acetylene ligand in **6** is not oriented parallel to a P-M-P vector. This difference is probably due to intramolecular packing forces, which minimize steric interactions between the bulky triisopropylsilyl and dmpe methyl groups. The most remarkable feature seen in the crystal structure of **6** is the asymmetric manner in which the acetylene is coordinated to tantalum. There is a 0.048-Å difference between the bond lengths for Ta-C1 and Ta-C2 and a 20.7° difference between C2-O2-Si2 and C1-O1-Si1.

The ^{31}P and ^{13}C NMR spectra and the ν_{CC} (or ν_{CO}) stretching frequency at 1555 cm^{-1} observed in the FTIR spectrum of **6** (Figure 3C) are analogous to those seen in the bis(trimethylsiloxy)acetylene complexes [M($Me_3SiOCCOSiMe_3$)$(dmpe)_2X$] (M = Ta, X = Cl, OTf; M = Nb, X = Cl) reported previously.[8] The ^{31}P and ^{13}C solution NMR spectra of ^{13}C-enriched **6** are displayed in Figure 7. The ^{13}C{^{1}H} NMR spectrum consists of two doublets of quintets (J_{PC} = 11, J_{CC} = 6 Hz) at 204 and 210 ppm. The phosphorus resonance is a triplet at 25.6 ppm (J_{PC} = 11 Hz). These results indicate that, at room temperature, the acetylene is freely rotating about the line extending from the Ta-Cl bond axis. The rotation barrier is very small, as evidenced by the lack of spectral change upon cooling of the sample to -89 °C.

Discussion

Two intermediates in the reductive coupling of carbon monoxide bound to seven-coordinate tantalum and niobium complexes (eq 3) have been isolated and structurally characterized. Additional mechanistic studies have provided clues to the nature of a third possible intermediate, or transition state, that has not been isolated.

The initial step in the pathway leading to reductive coupling is two-electron reduction of the dicarbonyl complex [$Ta(CO)_2(dmpe)_2Cl$] (**1**), yielding the anionic species [$Ta(CO)_2(dmpe)_2$]$^-$ (**3a** or **3b**). The C≡O stretching bands seen in the infrared spectrum of the sodium salt appear at 1663 and 1561 cm^{-1}, much lower in energy than those observed for Na[$Ta(CO)_6$] (1874 and 1835 cm^{-1})[22] owing to the electron-donating properties of the dmpe ligands. The [$Ta(CO)_2(dmpe)_2$]$^-$ anion has been isolated and structurally characterized as the tetra-*n*-hexylammonium salt. The sodium salt of the anion (**3a**) has been previously reported[10a] to form in the reaction of **1** with 2 equiv of sodium naphthalenide, as indicated in eq 4. Although the ^{31}P NMR spectrum of **3a** matches that reported in the

(22) Dewey, C. G.; Ellis, J. E.; Fjare, K. L.; Pfahl, K. M.; Warnock, G. F. P. *Organometallics* **1983**, *2*, 388.

$$[\underset{\mathbf{1}}{Ta(CO)_2(dmpe)_2Cl}] \xrightarrow{2Na(naphth)} Na[\underset{\mathbf{3a}}{Ta(CO)_2(dmpe)_2}] + NaCl + 2(naphthalene) \quad (4)$$

literature, its infrared spectrum contains two CO stretching frequencies, at 1663 and 1561 cm^{-1}, whereas only one such band, at 1675 cm^{-1}, was reported previously.[10a] Perhaps the lower energy band was observed but, owing to its low frequency, not identified as ν_{CO}.

Attempts to isolate a possible one-electron reduction product of **1** have thus far been unsuccessful. As shown in eq 5, reduction of **1** with 1 equiv of sodium naphthalenide yields a 1:1 mixture of **3a** and **1**. Although many

$$[\underset{\mathbf{1}}{Ta(CO)_2(dmpe)_2Cl}] + 1Na(naphth) \rightarrow \tfrac{1}{2}Na[\underset{\mathbf{3a}}{Ta(CO)_2(dmpe)_2}] + \tfrac{1}{2}[\underset{\mathbf{1}}{Ta(CO)_2(dmpe)_2Cl}] + naphthalene + \tfrac{1}{2}NaCl \quad (5)$$

neutral complexes of the type $[V(CO)_nL_{6-n}]$, where L is a neutral two-electron-donating ligand, have been reported,[23] the only analogous tantalum or niobium complex is $[Ta(CO)_6]$,[24] which has been observed in an argon matrix at 4.2 K. It is likely, therefore, that if the complex $[Ta(CO)_2(dmpe)_2]$ were formed in the reaction of **1** with 1 equiv of sodium naphthalenide, it would disproportionate as shown in eq 6.

$$2[\underset{\mathbf{3a}}{Ta(CO)_2(dmpe)_2}] + NaCl \rightarrow Na[\underset{\mathbf{3a}}{Ta(CO)_2(dmpe)_2}] + [\underset{\mathbf{1}}{Ta(CO)_2(dmpe)_2Cl}] \quad (6)$$

It is noteworthy that initial two-electron reduction of the kind indicated in eq 4 is also involved in the reductive coupling of two isocyanides in the complexes $[M(CNR)_6X]^+$ (M = W, Mo; X = Cl, Br, I, cyanide; R = alkyl) and $[Mo(CNR)_5(bipy)]^{2+}$.[25] It has recently been found in our laboratories that addition of aqueous HCl to a solution of the neutral molybdenum(0) complex $[Mo(CN\text{-}t\text{-}Bu)_6]$, formed by two-electron reduction of $[Mo(CNR)_6X]^+$, yields the reductively coupled product $[Mo(t\text{-}BuHNC{\equiv}CNH\text{-}t\text{-}Bu)(CN\text{-}t\text{-}Bu)_4Cl]^+$, eq 7.[26] When the technetium or

$$[Mo(CN\text{-}t\text{-}Bu)_6I]^+ \xrightarrow{2e^-} [Mo(CN\text{-}t\text{-}Bu)_6] \xrightarrow{2HI} [Mo(t\text{-}BuHNC{\equiv}CNH\text{-}t\text{-}Bu)(CN\text{-}t\text{-}Bu)_4I]^+ \quad (7)$$

rhenium complexes $[M(CN\text{-}t\text{-}Bu)_6X]^{2+}$ are subjected to conditions similar to those used to effect reductive coupling in the tungsten or molybdenum analogues (eq 7), the products isolated have undergone a two-electron reduction,[27] as shown in eq 8. These complexes do not react further with HX to undergo reductively coupling, presumably because there is insufficient electron density at the metal center.

$$[M(CNR)_6X]^{2+} + Zn(s) + H_2O \rightarrow [M(CNR)_6]^+ \quad (8)$$

(M = Tc or Re)

The next step identified in the CO reductive coupling mechanism is reaction of trialkylsilyl chloride with the $[Ta(CO)_2(dmpe)_2]^-$ anion to yield a trialkylsiloxycarbyne. This reaction can be envisioned as occurring via electrophilic attack by the trialkylsilyl reagent on one of the carbonyl oxygen atoms. The participation of this siloxycarbyne complex as an intermediate along the mechanistic pathway leading to reductive coupling is evidenced by the subsequent reaction of **4** with 1 equiv of Me_3SiCl to yield the asymmetric reductively coupled complex $[Ta\{Me_3SiOCCOSi(i\text{-}Pr)_3\}(dmpe)_2Cl]$. The siloxycarbyne complex **4** does not, however, undergo reductive coupling upon addition of a second equivalent of $(i\text{-}Pr)_3SiCl$, as indicated by phosphorus NMR studies. Perhaps the large steric requirements of the two triisopropylsilyl groups in the anticipated product preclude its formation. Spectroscopic characterization of **4** and the Nb analogue **5** indicates that the geometries found in the solid state are retained in solution. To our knowledge, compounds **4** and **5** are the first examples of such species, although there has been some theoretical work postulating that a similar reaction may be involved in Fischer–Tropsch chemistry (i.e., $MC{\equiv}O \rightarrow M{\equiv}COH$).[28] Work by Angelici and Greaves has shown that a thiocarbonyl may be converted into an alkylthiocarbyne by addition of electrophilic alkyl halides to electron-rich thiocarbonyl complexes,[29] as illustrated in eq 9.

$$[(HBpz_3)W(CO)_2(CS)]^- \xrightarrow{RX} [(HBpz_3)W(CO)_2(\equiv CSR)] \quad (9)$$

R = 2,4-dinitrophenyl, Me, Et; X = Cl, I

There are also many examples in the literature where electron-rich isocyanide complexes have been converted to aminocarbynes via electrophilic attack at nitrogen either by protons or alkyl groups.[30] One reaction of this kind was recently discovered in our laboratories during an attempt to extend the reductive coupling on molybdenum and tungsten to isoelectronic rhenium isocyanide complexes. Two of the isocyanide ligands in $[Re(CNR)_6X]^{2+}$ were replaced by phosphines in order to increase the electron density at the rhenium center. As mentioned previously, such a deficiency in electron density was believed to be one reason why the isocyanide ligands in $[Re(CNR)_6X]^{2+}$ would not reductively couple. When the complex $[Re(CN\text{-}t\text{-}Bu)_3(PMePh_2)_2Cl_2]^+$ was exposed to the same conditions that afforded reductively coupled products from $[M(CNR)_6X]^+$ (M = W, Mo), however, the aminocarbyne complex $[Re(\equiv CNH\text{-}t\text{-}Bu)(CN\text{-}t\text{-}Bu)_2(PMePh_2)_2Cl]^+$ was formed (eq 10).[9,31] This aminocarbyne

$$[Re(CN\text{-}t\text{-}Bu)_3(PMePh_2)_2Cl_2]^+ \xrightarrow[ZnCl_2\ (cat)]{Zn(s),\ H_2O} [Re(\equiv CNH\text{-}t\text{-}Bu)(CN\text{-}t\text{-}Bu)_2(PMePh_2)_2Cl]^+ \quad (10)$$

(23) Srivastava, S. C.; Shirmal, A. K. *Polyhedron* **1988**, *7*, 1639.
(24) Dekock, R. L. *Inorg. Chem.* **1971**, *10*, 1205.
(25) (a) Lam, C. T.; Corfield, P. W. R.; Lippard, S. J. *J. Am. Chem. Soc.* **1977**, *99*, 617. (b) Corfield, P. W. R.; Baltusis, L. M.; Lippard, S. J. *Inorg. Chem.* **1981**, *20*, 922. (c) Dewan, J. C.; Giandomenico, C. M.; Lippard, S. J. *Inorg. Chem.* **1981**, *20*, 4069. (d) Giandomenico, C. M.; Lam, C. T.; Lippard, S. J. *J. Am. Chem. Soc.* **1982**, *104*, 1263. (e) Caravana, C.; Giandomenico, C. M.; Lippard, S. J. *Inorg. Chem.* **1982**, *21*, 1860. (f) Hoffmann, R.; Wilker, C. N.; Lippard, S. J.; Templeton, J. L.; Brower, D. J. *J. Am. Chem. Soc.* **1983**, *105*, 146. (g) Warner, S.; Lippard, S. J. *Organometallics* **1986**, *5*, 1716.
(26) Carnahan, E. M.; Lippard, S. J. *J. Chem. Soc., Dalton Trans.*, in press.
(27) Farr, J. P.; Abrams, M. J.; Costello, C. E.; Davison, A.; Lippard, S. J. *Organometallics* **1985**, *4*, 139.
(28) Nicholas, K. M. *Organometallics* **1982**, *1*, 1713.
(29) Greaves, W. W.; Angelici, R. J. *Inorg. Chem.* **1981**, *20*, 2983.
(30) (a) Chatt, J.; Pombeiro, A. J. L.; Richards, R. L.; Royston, G. H. D.; Muir, K. W.; Walker, R. *J. Chem. Soc., Chem. Commun.* **1975**, 708. (b) Pombeiro, A. J. L.; Richards, R. L. *Transition Met. Chem.* **1980**, *5*, 55. (c) Chatt, J.; Pombeiro, A. J. L.; Richards, R. L. *J. Chem. Soc., Dalton Trans.* **1980**, 492; **1979**, 1585. (d) Carvalho, M. F. N. N.; Pombeiro, A. J. L.; Schubert, U.; Orama, O.; Pickett, C. J.; Richards, R. L. *J. Chem. Soc., Dalton Trans.* **1985**, 2079. (e) Carvalho, M. F. N. N.; Laranjeira, C. M. C.; Nobre, A. T. Z.; Pombeiro, A. J. L.; Richards, R. L. *Transition Met. Chem.* **1985**, *10*, 427. (f) Singleton, E.; Oosthuizen, H. E. *Adv. Organomet. Chem.* **1983**, *22*, 292. (g) Pombeiro, A. J. L.; Carvalho, M. F. N. N.; Hitchcock, P. B.; Richards, R. L. *J. Chem. Soc., Dalton Trans.* **1981**, 1629. (h) Pombeiro, A. J. L.; Hughes, D. L.; Pickett, C. J.; Richards, R. L. *J. Chem. Soc., Chem. Commun.* **1986**, 246. (i) Chiu, K. W.; Howard, C. G.; Wilkinson, G.; Galas, A. M.; Hursthouse, M. B. *Polyhedron* **1982**, *1*, 803.

Scheme I

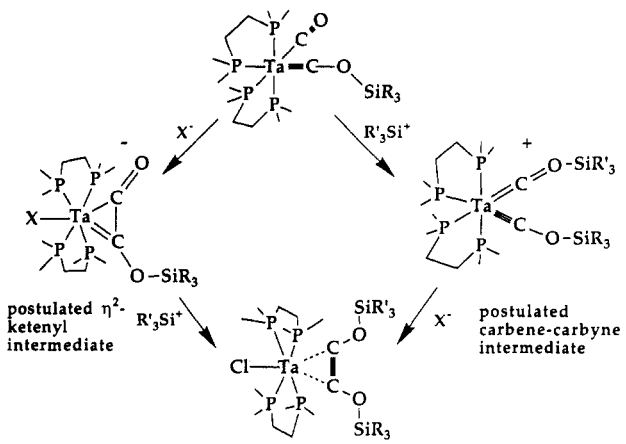

probably arises from initial two-electron reduction of the starting material yielding $[Re(CN\text{-}t\text{-}Bu)_3(PMePh_2)_2Cl]$, which then reacts with HCl to generate the observed product.[9,31]

The next step in the reductive coupling reaction, transformation of the siloxycarbyne into the final bis(trialkylsiloxy)acetylene complex, can proceed via two possible intermediates as shown in Scheme I. There are many examples of carbyne–CO coupling in the literature.[32] Almost all such coupling reactions are known, or believed, to proceed via an η^2-ketenyl intermediate.[32a-h] There is, however, a report[32i] in which the coupling of a terminal carbonyl with a carbyne is postulated to occur via a bis(carbyne) intermediate, as shown in eq 11. Such a process

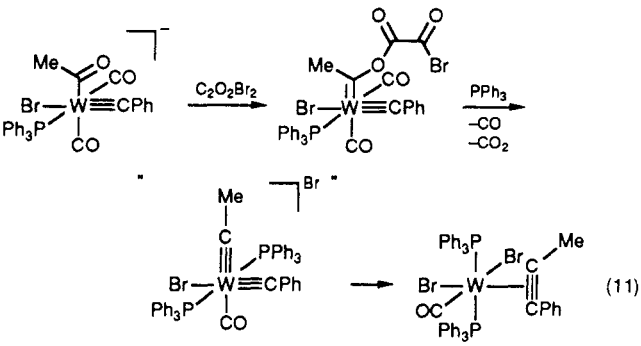

(11)

is symmetry allowed for group 6 metal complexes.[33] The existence of such a bis(carbyne) intermediate, however, has not been demonstrated. It may be that formation of an η^2-ketenyl transition state promotes expulsion of CO_2 and CO and that the reaction does not proceed through a bis(carbyne) intermediate. An analogous bis(carbyne) species has recently been postulated to be involved in the reductive coupling of a carbyne with an isocyanide in the tungsten complex, $[W(\equiv CPh)(CN\text{-}t\text{-}Bu)_4X]$, although no supporting evidence was provided.[34]

Studies were undertaken in an attempt to distinguish between the possible η^2-ketenyl and carbene–carbyne intermediates illustrated in Scheme I. If an η^2-ketenyl transition state were involved in the mechanism, the overall reaction would be favored by silyl reagents in which the halide is a good nucleophile. This choice would facilitate nucleophilic attack at the metal center to form the η^2-ketenyl species. If the reaction proceeded via carbene–carbyne coupling, it would be accelerated by a silyl halide reagent having a highly polarized Si–X bond to facilitate electrophilic attack at the carbonyl oxygen by the trialkyl silyl group.

Addition of 1 equiv of Me_3SiCl to a solution of $(n\text{-}C_6H_{13})_4N[Ta(CO)_2(dmpe)_2]$ (**3b**) in THF yielded the corresponding trimethylsiloxycarbyne complex $[Ta(\equiv COSiMe_3)(CO)(dmpe)_2]$, as evidenced by ^{31}P NMR spectroscopy. When, on the other hand, Me_3SiI was substituted for Me_3SiCl under the same reaction conditions, a 1:1 mixture of the coupled product $[Ta(Me_3SiOCCOSiMe_3)(dmpe)_2I]$ and unreacted **3b** was observed in the ^{31}P NMR spectrum of the final products. This observation in itself does not distinguish between the intermediacy of an η^2-ketenyl or a carbene–carbyne species, since Me_3SiI provides both a good nucleophile (I^-) and a highly polarized Si–I bond. It was also observed, however, that when 1 equiv of Me_3SiOTf is added to a solution of **3b** in dimethoxyethane, the only product seen in the ^{31}P NMR spectrum was the trimethylsiloxycarbyne complex, as found for the reaction involving addition of Me_3SiCl. Since Me_3SiOTf has a very polarized Si–OTf bond but does not provide a good nucleophile, this triad of experiments supports the pathway involving an η^2-ketenyl transition state. In such a high-coordinate species, the nonbonded C···C distance would be shortened, facilitating coupling as anticipated previously.[8]

The synthesis and structural characterization of the asymmetrically coupled product $[Ta\{Me_3SiOCCOSi(i\text{-}Pr)_3\}(dmpe)_2Cl]$ (**6**), formed by reaction of **4** with Me_3SiCl, supports the assignment of the siloxycarbyne as an intermediate in the C–C coupling reaction mechanism. Moreover, complex **6** allowed us to determine whether the coordinated acetylene ligand is freely rotating in solution. The $^{13}C\{^1H\}$ NMR spectrum of 90% ^{13}C-enriched **6** exhibits two carbon resonances, split by one another as well as by four equivalent phosphines. This result indicates free rotation of the coordinated disiloxyalkyne. The barrier to rotation is very small, as revealed by the inability to obtain a spectrum corresponding to the solid-state structure at temperatures down to −98 °C. In related work,[35] the barrier to rotation of the acetylene ligand in $[Ta(CO)_2(PhCCH)(PMe_3)_2I]$ was found to be 16 kcal/mol. The structure of this complex is similar to that of **6**, with the two equatorial dmpe groups being replaced by two trans pairs of phosphine and carbonyl ligands. The most energetically stable orientation of the phenylacetylene in $[Ta(CO)_2(PhCCH)(PMe_3)_2I]$ is in parallel alignment to the two trans carbonyls, a conformation partially due to enhanced electronic interactions and partially to steric interactions. In the case of the reductively coupled bis(trialkylsiloxy)acetylene product **6**, where the equatorial plane consists of four identical phosphorus donor atoms, there may not be as large an electronic and steric preference for one alignment over another, and the energy barrier

(31) Warner, S.; Lippard, S. J. *Organometallics* **1989**, *8*, 228.
(32) (a) James, A. P.; Stone, F. G. A. *J. Organomet. Chem.* **1986**, *310*, 47. (b) Birdwhistell, K. R.; Tonker, T. L.; Templeton, J. L. *J. Am. Chem. Soc.* **1985**, *107*, 4474. (c) Kreissl, F. R.; Sieber, W. J.; Wolfgruber, M. *Z. Naturforsch.* **1983**, *38b*, 1419. (d) Mayr, A.; McDermott, G. A.; Dorries, A. M.; Van Engen, D. *Organometallics* **1987**, *6*, 1503. (e) Churchill, M. R.; Wasserman, H. J.; Holmes, S. J.; Schrock, R. R. *Organometallics* **1982**, *1*, 766. (f) Fischer, E. O.; Friedrich, P. *Angew. Chem., Int. Ed. Engl.* **1979**, *18*, 327. (g) Sheridan, J. B.; Geoffroy, G. L.; Rheingold, A. L. *Organometallics* **1986**, *5*, 1514. (h) Chisholm, M. H.; Ho, D.; Huffman, J. C.; Marchant, N. S. *Organometallics* **1989**, *8*, 1626. (i) McDermott, G. A.; Mayr, A. *J. Am. Chem. Soc.* **1987**, *109*, 580.
(33) Hoffmann, R.; Wilker, C. N.; Eisenstein, O. *J. Am. Chem. Soc.* **1982**, *104*, 632.
(34) (a) Filippou, A. C.; Grünleitner, W. *Z. Naturforsch.* **1989**, *44b*, 1023. (b) Filippou, A. C.; Völkl, C.; Grünleitner, W.; Kiprof, P. *Angew. Chem., Int. Ed. Engl.* **1990**, *29*, 207.
(35) McGeary, M. J.; Gamble, A. S.; Templeton, J. L. *Organometallics* **1988**, *7*, 271.

Scheme II

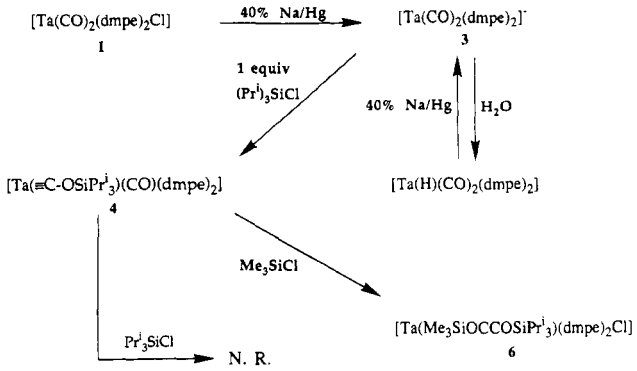

Scheme III

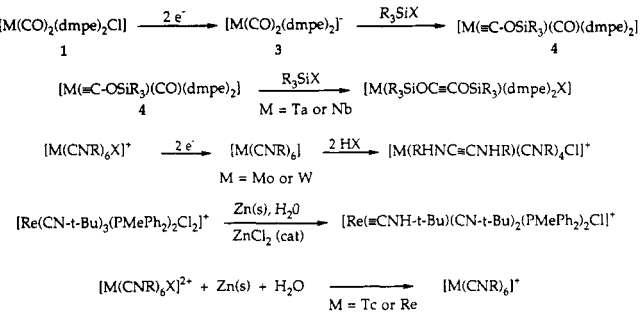

to rotation of the acetylene is correspondingly lowered. Indeed, if we assume the separation between phosphorus signals in the nonrotating frame to be between 0.1 and 1.0 ppm (12.1 and 121 Hz) at −98 °C, then we can put an upper limit on the barrier to rotation of 7.8–8.7 kcal/mol.

Conclusions

The mechanism by which two carbon monoxide ligands bound to the seven-coordinate tantalum or niobium complexes $[M(CO)_2(dmpe)_2Cl]$ [M = Ta (**1**), Nb (**2**)] are reductively coupled has been explored. Experimental and theoretical studies support the scheme outlined in Scheme II. The reaction proceeds by initial two-electron reduction, affording the $[M(CO)_2(dmpe)_2]^-$ anion in which the carbonyl ligands are cis to one another. Formation of this species is followed by electrophilic attack by a trialkylsilyl halide on one of the carbonyl oxygen atoms, yielding the neutral siloxycarbyne $[Ta(\equiv COSiR_3)(CO)(dmpe)_2]$. The transition state in the reaction pathway between this siloxycarbyne and the final coupled product appears to traverse an η^2-ketenyl complex, although such a species has not been isolated or spectroscopically identified.

The mechanistic evidence gained from the present studies of reductive coupling of CO on tantalum and niobium complexes has led us to reconsider the analogous reductive coupling of isocyanides in an effort to determine whether a common mechanism might be involved. Scheme III summarizes the results obtained in our laboratory during attempts to couple CO or isocyanides reductively on various metal complexes. As indicated, reductive coupling of isocyanides in the molybdenum complex $[Mo(CN\text{-}t\text{-}Bu)_6X]^+$ proceeds through an initial two-electron reduction step, yielding a neutral complex $[Mo(CN\text{-}t\text{-}Bu)_6]$ isoelectronic with **3** (**a** and **b**). Reaction of $[Mo(CN\text{-}t\text{-}Bu)_6]$ with aqueous HI affords the reductively coupled product $[Mo(t\text{-}BuHNCCNH\text{-}t\text{-}Bu)(CN\text{-}t\text{-}Bu)_4I]^+$.[26] An analogous two-electron reduction also occurs when the technetium or rhenium complexes $[M(CNR)_6X]^{2+}$ are exposed to conditions that promote reductive coupling of isocyanides in the isomorphous and isoelectronic $[M(CNR)_6X]^+$ (M = W, Mo) complexes. In the case of the rhenium and technetium complexes, the two-electron-reduction product $[M(CNR)_6]^+$ (M = Tc, Re) forms but does not react further. The complex $[Re(CN\text{-}t\text{-}Bu)_3(PMePh_2)_2Cl_2]^+$ was exposed to the same conditions as the previous rhenium complexes, with the expectation that increased σ donation from the phosphine ligands would increase the level of electron density at the metal center and thus promote reductive coupling. The product obtained from this reaction, however, was the aminocarbyne complex $[Re(\equiv CNH\text{-}t\text{-}Bu)(CN\text{-}t\text{-}Bu)_2(PMePh_2)_2Cl]^+$, which is isoelectronic with the siloxycarbyne complexes $[M(\equiv COSiR_3)(CO)(dmpe)_2]$, M = Ta (**4**) or Nb (**5**).

Both reductive coupling of CO on tantalum or niobium and of alkyl isocyanides on molybdenum or tungsten thus appear to occur by the same or similar mechanism. In principle, such a reaction pathway should be available to couple reductively other linear, triply bonded substrates (e.g., CO, CNR, N_2^-, CCR, etc.). All that is required are the correct metal–ligand system, reducing agent, and Lewis acid. Research in this area is currently under investigation and has recently led to the cross-coupled product $[Nb(Me_3SiOC\equiv CN(Me)SiMe_3)(dmpe)_2Cl]$, obtained by coupling of CO with MeNC in $[Nb(CO)(CNMe)(dmpe)_2Cl]$.[36]

Acknowledgment. We are grateful to the National Science Foundation for support of this research and to E. M. Carnahan and Dr. W. M. Davis for helpful discussions.

Supplementary Material Available: Tables S1–S3, S5–S7, S9–S11, and S13–S15, listing atomic coordinates and thermal parameters for compounds **3b** and **4–6** (22 pages); Tables S4, S8, S12, and S16, listing observed and calculated structure factor amplitudes for compounds **3b** and **4–6** (139 pages). Ordering information is given on any current masthead page.

(36) Carnahan, E. M.; Lippard, S. J. *J. Am. Chem. Soc.* **1990**, *112*, 3230.